Reac Kinet Mech Cat (2014) 112:27–36
DOI 10.1007/s11144-014-0688-0

Influence of the preparation method on the performance of CeO_2–MoO_3 catalyst for the selective catalytic reduction of NO with NH_3

Xiaoliang Li · Yonghong Li

Received: 15 December 2013 / Accepted: 8 February 2014 / Published online: 22 February 2014

Abstract CeO_2–MoO_3 catalysts were prepared by three methods: single step sol–gel, homogeneous precipitation, hydrothermal. These catalysts were used for the selective catalytic reduction of NO with NH_3 in the temperature range from 150 to 400 °C. The tested results suggested that the catalyst prepared by the hydrothermal method showed the higher NO conversion. The BET, XRD, H_2-TPR, NH_3-TPD and in situ DRIFTS characterization results indicated that the larger surface area, highly dispersed nanoctrystalline ceria, good redox ability and the stronger adsorption capacity for the NH_3 should be the key factors to acquire the better NH_3-SCR performance.

Keywords Prepared method · Characterization · Selective catalytic reduction · NH_3

Introduction

Nitrogen oxides (NO_x) can result in acid rain, photochemical smog, ozone depletion and endangering human health [1]. Selective catalytic reduction of NO_x with NH_3 (NH_3-SCR) is the most effective method to control NO_x emissions and the corresponding commercial catalysts for this reaction process are V_2O_5–WO_3 (MoO_3)/TiO_2 [2]. However, some drawbacks still exist in this catalyst system, such

X. Li · Y. Li (✉)
Key Lab for Green Chemical Technology of Ministry of Education, School of Chemical Engineering and Technology, Tianjin University, Weijin Road 92, Tianjin 300072, China
e-mail: yhli@tju.edu.cn

Y. Li
National Engineering Research Center for Distillation Technology, Tianjin 300072, China

as the narrow operation temperature window (300–400 °C), low N_2 selectivity at high temperatures and high toxicity of vanadium species [3–5]. Therefore, developing an environmentally friendly NH_3-SCR catalyst with excellent catalytic activity and low N_2O formation in a broad temperature scope has been concerned by many researchers.

Among all the reported vanadium-free catalysts, ceria based catalysts have been studied extensively and applied as NH_3-SCR catalysts due to their outstanding oxygen storage-release capacity and excellent redox properties. In recent years, CeO_2 mixed with other metal oxides such as MnO_x–CeO_2 mixed oxides [6], ceria modified MnO_x–TiO_2 [7], CeO_2–TiO_2 [8–10], CeO_2–WO_3 [11, 12], CeO_2–Al_2O_3 [13], Ce–W–Ti mixed oxide [14], Ce–Cu–Ti mixed oxide [15, 16], Ce–Sn–O_x catalyst [17], WO_3/ZrO_2–$Ce_{0.6}Zr_{0.4}O_2$ [18] and Nb doped MnO_x–CeO_2 catalyst [19] as superior NH_3-SCR catalysts have been reported by many researchers. Our group lately developed a promising Ce–Mo–O_x catalyst [20], which exhibited excellent activity and high SO_2/H_2O durability. Nevertheless, the catalyst preparation method can influence the catalytic performance and the interaction between the active components significantly. Therefore, it is necessary to carry out the comparison of the activity and characterization of the CeO_2–MoO_3 catalysts prepared by different methods.

In this study, CeO_2–MoO_3 catalysts were prepared by three methods with the optimal Ce/Mo molar ratio of 2:1 [20], namely, single step sol–gel (SG), homogeneous precipitation (HP), hydrothermal (HT). The main purpose of this investigation is to find an optimal method for preparing CeO_2–MoO_3 catalyst with the best NH_3-SCR catalytic performance.

Experimental

Catalyst preparations

Single step sol–gel method (SG)

All chemicals used were of analytical grade. $(NH_4)_6Mo_7O_{24}{\cdot}4H_2O$ with equal weight $H_2C_2O_4{\cdot}2H_2O$ were added into the deionized water. After the ammonium molybdate was dissolved completely $(NH_4)_2Ce(NO_3)_6$ and citric acid were added into the aqueous solution under vigorous stirring at room temperature, the pH of this solution was adjusted to 1.0 using dilute nitric acid. Then the mixed solution was slowly vaporized at 70 °C to yield a transparent colloidal solution, and then dried at 110 °C for 12 h to form xerogel, followed by calcination in static air at 500 °C for 5 h. Finally, the catalyst was crushed and sieved to 40–60 meshes for activity test.

Homogeneous precipitation method (HP)

$(NH_4)_6Mo_7O_{24}{\cdot}4H_2O$ with equal weight $H_2C_2O_4{\cdot}2H_2O$ were added to deionized water. After the dissolution of ammonium molybdate, the aqueous solution of

$(NH_4)_2Ce(NO_3)_6$ was added with the required molar ratio. Excessive urea aqueous solution was then added into the mixed solution, with a urea/(Ce+Mo) molar ratio being 20:1. The mixed solution was then heated at 90 °C for 12 h. The precipitated solids were collected by filtration and washed with deionized water, followed by drying at 110 °C for 12 h and subsequently calcination at 500 °C for 5 h in the static air atmosphere. Finally, the catalysts were crushed and sieved to 40–60 meshes for activity test.

Hydrothermal method (HT)

Appropriate amounts of $(NH_4)_6Mo_7O_{24}{\cdot}4H_2O$ with equal weight $H_2C_2O_4{\cdot}2H_2O$ were dissolved in deionized water at room temperature $(NH_4)_2Ce(NO_3)_6$ was added into the aqueous and stirred for 1 h, then excessive 25 wt% $NH_3{\cdot}H_2O$ solution was dropped into the mixed solution under vigorous agitation until pH 10. After stirring for 90 min, the obtained suspension was transferred into a Teflon-sealed autoclave and aged at 120 °C for 24 h. The obtained precipitate was filtered and washed with deionized water thoroughly. The resulting solid was dried at 110 °C for 12 h and then calcined in the static air at 500 °C for 5 h. Finally, the catalysts were crushed and sieved to 40–60 meshes for activity test.

To better interpret the characterization of the CeO_2–MoO_3 catalysts, pure CeO_2 and MoO_3 were also prepared by the direct decomposition method using $(NH_4)_2Ce(NO_3)_6$ and $(NH_4)_6Mo_7O_{24}{\cdot}4H_2O$ as precursors, respectively.

Characterization of catalysts

The Brunauer–Emmett–Teller (BET) results were measured by N_2 adsorption at 77 K using a Micromeritics Tristar-3000 system. Prior to the N_2 physisorption, catalysts were degassed at 300 °C for 4 h. Surface areas were determined by the BET equation in the 0.05–0.35 partial pressure range.

The X-ray diffraction (XRD) patterns were recorded on a Rigaku D/max 2500 with Cu K_α radiation, scanning between 10° and 80° at a step of 5°/min.

Hydrogen temperature programmed reduction (H_2-TPR) and NH_3-temperature programmed desorption (NH_3-TPD) profiles were carried out by using a Micromeritics Auto Chem II 2920 instrument. For the H_2-TPR, in each experiment, a 50 mg sample was loaded into the quartz reactor and pretreated in He (50 mL/min) at 300 °C for 1 h. The sample was then cooled to room temperature under flowing He. The sample was reduced starting at room temperature and increasing up to 900 °C in a gas mixture of 10 % H_2/He at 10 °C/min. The consumption of H_2 was monitored continuously using a thermal conductivity detector. For the NH_3-TPD experiments, after pretreatment in a He stream at 200 °C for 1 h, the catalysts were cooled down to 50 °C and saturated with NH_3 at a flow rate of 40 mL/min for 1 h, followed by flushing with He at 100 °C to avoid physisorption of NH_3. Desorption was carried out by heating the catalyst in He from 100 to 550 °C with a heating rate of 10 °C/min.

The in situ DRIFTS experiments were performed on a FT-IR (Fourier transform infrared) spectrometer (Nicolet Nexus 670) equipped with an in situ diffuse

reflection chamber and high sensitivity mercury–cadmium–telluride (MCT) detector cooled by liquid nitrogen. An about 30 mg sample was finely ground and placed in the in situ chamber. The mass flow controllers and temperature controller were used to simulate the reaction conditions. Prior to each experiment, the catalyst was heated at 500 °C for 30 min in a flow of 10 % O_2/N_2 and then cooled to 200 °C. The background spectrum was recorded and subtracted from the sample spectrum. All the spectra were collected with an accumulating 100 scans at a resolution of 4 cm^{-1}.

Activity test

The SCR activity measurements were carried out in a fixed bed quartz reactor (inner diameter 10 mm) under atmospheric conditions. A K-type thermocouple (o.d. 1 mm) was directly immersed into the catalyst bed from the bottom of the reactor and connected to a programmable temperature controller to monitor the reaction temperature. The composition of the model flue gas was: 500 ppm NO, 500 ppm NH_3, 5 % O_2, balance N_2, and 300 mL/min total flow rate, yielding a GHSV of 50,000 h^{-1}. The concentrations of NO and NO_2 in the inlet and outlet gas were measured by an online chemiluminescent NO/NO_x analyzer (Model KM9106, Kane Inc). The N_2O concentration was analyzed by a gas chromatograph (FULI 9790, Zhejiang Wenling Inc) with a porapak Q column. The data were collected after 1 h when the SCR reaction had reached a steady state. NO conversion and N_2O selectivity were calculated as following [21]:

$$\text{NO conversion} = \frac{[\text{NO}_x]_{\text{inlet}} - [\text{NO}_x]_{\text{outlet}}}{[\text{NO}_x]_{\text{inlet}}} \times 100\ \%; \quad \text{with } [\text{NO}_x] = [\text{NO}] + [\text{NO}_2]$$

$$\text{N}_2\text{O selectivity} = \frac{2[\text{N}_2\text{O}]_{\text{outlet}}}{[\text{NO}_x]_{\text{inlet}} - [\text{NO}_x]_{\text{outlet}}} \times 100\ \%$$

Results and discussion

Catalytic activity tests

The NO conversions and N_2O selectivity versus reaction temperature using CeO_2–MoO_3 catalysts prepared by different methods in the NH_3-SCR reaction are shown in Fig. 1. As can be seen from the figure, the CeO_2–MoO_3 (HT) catalyst performed most efficiently in the enitre temperature range and an almost total NO conversion was achieved from 300 to 400 °C under the GHSV of 50,000 h^{-1}. Some N_2O was detected at above 350 °C, which hinted that the NH_3 oxidation reaction started. In the meanwhile, CeO_2–MoO_3 (HP) exhibited the similar catalytic activity to CeO_2–MoO_3 (HT) at high temperature. By contrast, the CeO_2–MoO_3 (SG) catalyst exhibited the lowest NO conversion and N_2O selectivity compared with the other two catalysts under the tested condition. Therefore, it can be seen that the catalytic performance was influenced evidently by the catalyst preparation method.

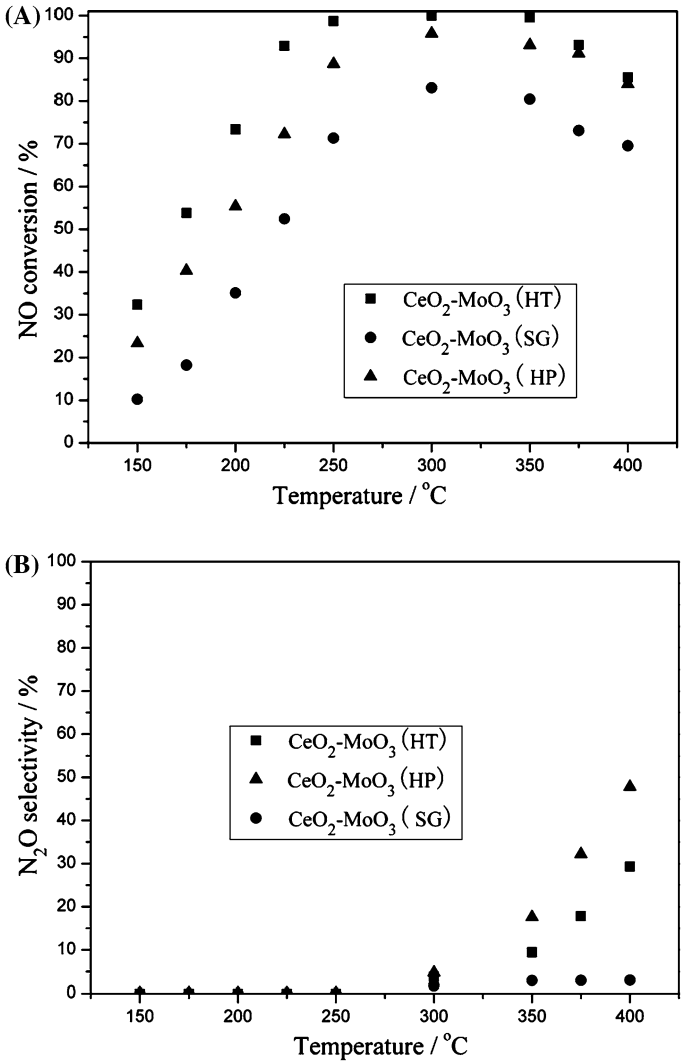

Fig. 1 NO conversion and N_2O selectivity over CeO_2–MoO_3 (HT), CeO_2–MoO_3 (HP) and CeO_2–MoO_3 (SG) catalysts under GHSV of 50,000 h^{-1}

Characterization of catalysts

XRD and BET

The XRD patterns of the CeO_2–MoO_3 catalysts prepared by different methods are shown in Fig. 2. Obviously, the cerianite CeO_2 phase could be detected on the catalysts, yet no diffraction peaks attributed to MoO_3 could be found, which indicated that MoO_3 existed mainly in amorphous state or mostly in highly

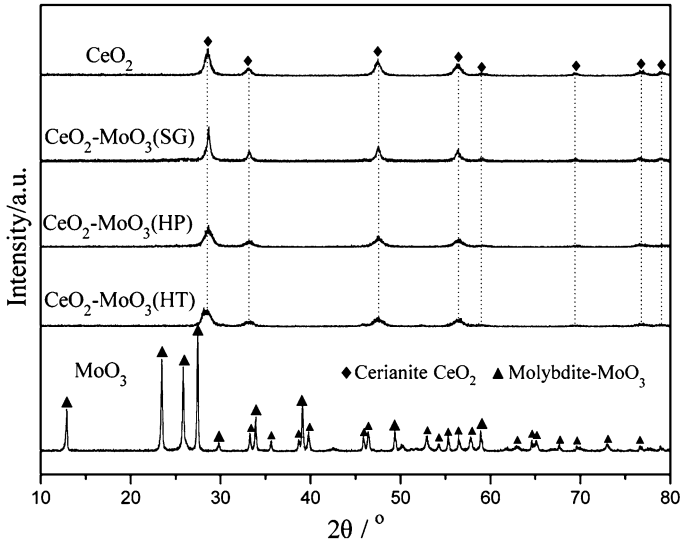

Fig. 2 XRD patterns of the CeO_2–MoO_3 (HT), CeO_2–MoO_3 (HP) and CeO_2–MoO_3 (SG) catalysts

Table 1 BET surface area and CeO_2 crystallite size of the catalysts

Sample	BET surface area (m^2/g)	Crystallite size of CeO_2[a] (nm)
CeO_2–MoO_3 (SG)	15	16.2
CeO_2–MoO_3 (HP)	25	9.5
CeO_2–MoO_3 (HT)	38	8.9

[a] CeO_2 crystallite size calculated by the Scherrer equation from XRD results

dispersed state in the CeO_2–MoO_3 catalysts. It also could be seen that the intensity of the CeO_2 peak on the CeO_2–MoO_3 (HT) was the smallest. Meanwhile, the mean crystallite size of CeO_2 in the CeO_2–MoO_3 catalysts was calculated by using the Scherrer equation, and the corresponding results are displayed in Table 1. Clearly, the CeO_2–MoO_3 (HT) catalyst owned the smallest crystallite size of CeO_2 among these three CeO_2–MoO_3 samples, which were consistent with the XRD results.

The BET results of the CeO_2–MoO_3 catalysts prepared by different methods are exhibited in Table 1. It can be seen from the table that the CeO_2–MoO_3 (HT) possessed the maximal surface area and the CeO_2–MoO_3 (SG) showed the smallest one. Therefore, different preparation methods can result in the different physical structure of the catalysts. Similar phenomena have been reported by Gao et al. [15] when they prepared the CeO_2/TiO_2 catalysts using different methods.

H_2-TPR

The reducibility of the catalysts is an important factor to affect the SCR reaction activity [22]. The reducibilities of the CeO_2, MoO_3 and CeO_2–MoO_3 catalysts were

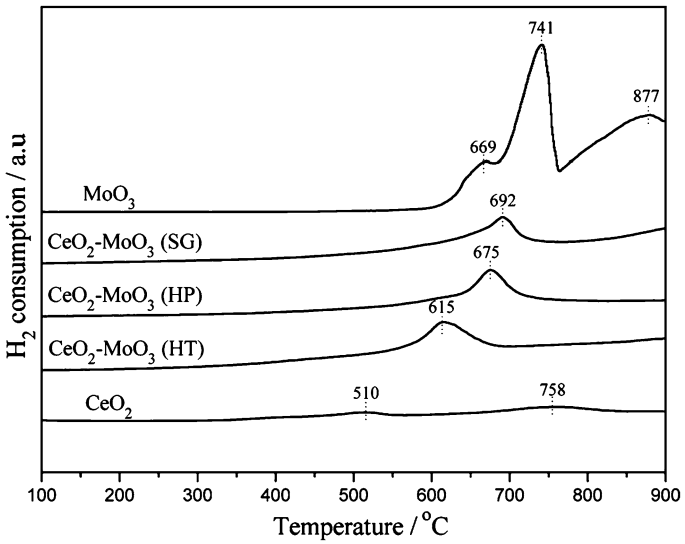

Fig. 3 H_2-TPR profiles of the CeO_2–MoO_3 (HT), CeO_2–MoO_3 (HP) and CeO_2–MoO_3 (SG) catalysts

characterized by H_2-TPR experiments and the corresponding results are shown in Fig. 3. As seen in the figure, the TPR profile of the CeO_2 showed two reduction peaks, the first peak at 510 °C corresponded to the reduction of surface Ce^{4+} to Ce^{3+}, and the peak at higher temperature could be attributed to the reduction of bulk CeO_2 [23]. The TPR profile of the MoO_3 displayed three peaks, the peaks at 669 and 741 °C could be attributed to the reduction from MoO_3 to MoO_2 and the peak at 877 °C could be attributed to the reduction from MoO_2 to Mo [24]. It could be also noted that the position of the CeO_2 reduction peak shifted to the different higher temperatures in the CeO_2–MoO_3 catalysts prepared by different methods and no reduction peak attributed to molybdenum oxides species could be detected in the measured temperature range. Meanwhile, the reduction peak belonged to the CeO_2–MoO_3 catalysts showed a higher area than that of CeO_2, which hinted that the redox ability was improved markedly by mixing with Mo. Among these three CeO_2–MoO_3 catalysts, the CeO_2–MoO_3 (HT) displayed the lowest reduction temperature, which indicated that the CeO_2–MoO_3 (HT) catalyst had the best redox ability. At the same time, the peaks attributed to the CeO_2–MoO_3 (HP) and CeO_2–MoO_3 (SG) catalysts showed at higher temperatures and the area of the reduction peaks became smaller, which suggested that the redox activity was reduced. All of these analysis proved that the interaction between Ce and Mo species in the CeO_2–MoO_3 catalyst was affected by the different preparation method.

NH_3-TPD

Apart from the reducibility of the catalyst, the surface acidity is also a key factor to influence the NH_3-SCR reaction performance of the catalyst [25]. The NH_3-TPD

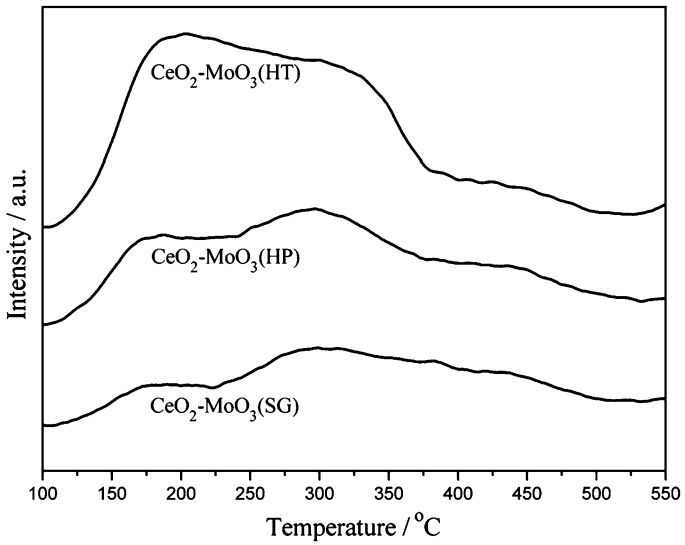

Fig. 4 NH_3-TPD curves of the CeO_2–MoO_3 (HT), CeO_2–MoO_3 (HP) and CeO_2–MoO_3 (SG) catalysts

curves of the CeO_2–MoO_3 catalysts prepared by different methods are displayed in Fig. 4. As shown in the figure, the desorption peaks of the CeO_2–MoO_3 (HT) catalyst occurred at 192 and 308 °C due to the desorption of weakly and strongly adsorbed NH_3, respectively. Correspondingly, the desorption peaks of the CeO_2–MoO_3 (HP) and CeO_2–MoO_3 (SG) catalysts are located at 177 and 299 °C, respectively. The NH_3 adsorption capacity sequence is following by: CeO_2–MoO_3 (HT) (234.5 μmoL/g) > CeO_2–MoO_3 (HP) (163.3 μmoL/g) > CeO_2–MoO_3 (SG) (103.2 μmoL/g). However, after normalization by the BET surface area, the density of the acid sites on the catalyst surface is almost the same (6 μmoL/g m^2). The above analysis results suggested that the catalysts prepared by the HT methods had the maximum BET area surface and further own much more surface acid sites, which played an important role to obtain the high NH_3-SCR performance.

In situ DRFTS

The DRIFTS spectra of the NH_3 adsorption for the CeO_2–MoO_3 catalysts at 200 °C are displayed in Fig. 5. As the in situ DRIFTS exhibits in the figure, the bands at 1,238/1,602 cm^{-1} can be attributed to the coordinated NH_3 on Lewis acid sites [26, 27], while the bands at 1,413/1,660 cm^{-1} can be assigned to ionic NH_4^+ species on Brønsted acid sites [26, 28]. In the N–H stretching region, three bands were found at 3173, 3260 and 3381 cm^{-1} [29]. Another negative band at 3,620 cm^{-1} was also detected [30], which could be assigned to the hydroxyl consumption. The DRIFTS spectra showed that the peak for the CeO_2–MoO_3 (HT) catalyst was very strong, especial the peak at 1,413 cm^{-1}, indicating that there were many acid sites on the catalyst surface, which was also consistent with the NH_3-TPD characterization

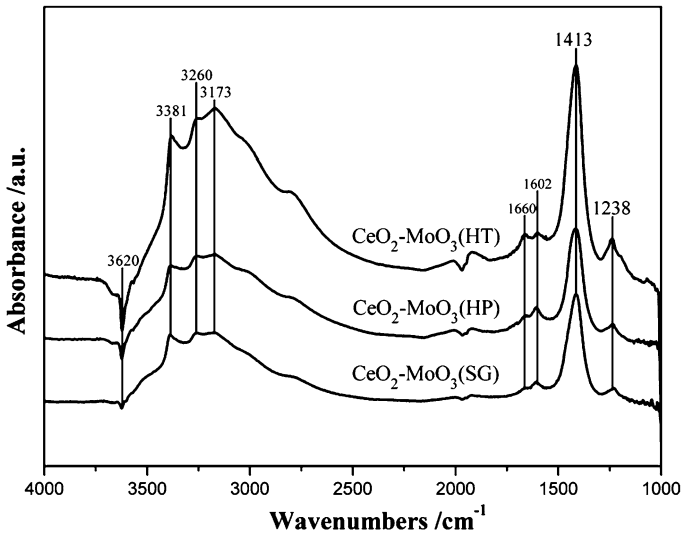

Fig. 5 In situ DRIFTS spectra of NH_3 adsorption on the CeO_2–MoO_3 (HT), CeO_2–MoO_3 (HP) and CeO_2–MoO_3 (SG) catalysts at 200 °C

result. However, the peaks attributed to the CeO_2–MoO_3 (SG) catalyst were the lowest, thus the NH_3 adsorption on the catalyst surface was influenced markedly by the preparation method.

Conclusion

Based on the above results, it can be concluded that the CeO_2–MoO_3 catalyst prepared by the hydrothermal method showed the best catalytic activity under our tested conditions. On the basis of the obtained characterization results, the good NH_3-SCR catalytic activity can be attributed to the larger surface area, highly dispersed nanoctrystalline ceria, good redox ability and the stronger adsorption capacity for the NH_3. All of these factors are affected by the preparation method.

Acknowledgments We acknowledge gratefully the financial support of the Program of Universities' Innovative Research Terms (No. IRT0936).

References

1. Bosch H, Janssen F (1988) Catal Today 2:369–521
2. Nova I, Lietti L, Casagrande L, Dall'Acqua L, Giamello E, Forzatti P (1998) Appl Catal B 17:245–258
3. Busca G, Lietti L, Ramis G, Berti F (1998) Appl Catal B 18:1–36
4. Liu F, He H, Zhang C, Shan W, Shi X (2011) Catal Today 175:18–25
5. Balle P, Geiger B, Kurten S (2009) Appl Catal B 85:109–119
6. Qi G, Yang RT, Chang R (2004) Appl Catal B 51:93–106

7. Wu Z, Jin R, Liu Y, Wang H (2008) Catal Commun 9:2217–2220
8. Xu W, Yu Y, Zhang C, He H (2008) Catal Commun 9:1453–1457
9. Gao X, Jiang Y, Fu Y, Zhong Y, Luo Z, Cen K (2010) Catal Commun 11:465–469
10. Shan W, Liu F, He H, Shi X, Zhang C (2011) ChemCatChem 3:1286–1289
11. Chen L, Li J, Ablikim W, Wang J, Chang H, Ma L, Xu J, Ge M, Arandiyan H (2011) Catal Lett 141:1859–1864
12. Shan W, Liu F, He H, Shi X, Zhang C (2011) Chem Commun 47:8046–8048
13. Shen Y, Zhu S, Qiu T, Shen S (2009) Catal Commun 11:20–23
14. Shan W, Liu F, He H, Shi X, Zhang C (2012) Chem Commun Appl Catal B 115–116:100–106
15. Gao X, Du X, Cui L, Fu Y, Luo Z, Cen K (2010) Catal Commun 12:255–258
16. Liu Z, Yi Y, Li J, Woo SI, Wang B, Cao X, Li Z (2013) Chem Commun 49:7726–7728
17. Li X, Li Y, Deng S, Rong TA (2013) Catal Commun 40:47–50
18. Baidya T, Bernhard A, Elsener M, Kröcher O (2013) Top Catal 56:23–28
19. Casapu M, Kröcher O, Elsener M (2009) Appl Catal B 88:413–419
20. Li X, Li Y (2014) Catal Lett. 144:165–171
21. Ma L, Li J, Arandiyan H, Shi W, Liu C, Fu L (2012) Catal Today 184:145–152
22. Du X, Gao X, Qu R, Ji P, Luo Z, Cen K (2012) ChemCatChem 12:2075–2081
23. Murugan B, Ramaswamy AV (2008) J Phys Chem C 112:20429–20442
24. Amoldy P, De Jonge JCM, Moulijo JA (1985) J Phys Chem 89:4517–4526
25. Topsφe NY (1994) Science 265:1217–1219
26. Yang S, Wang C, Chen J, Peng Y, Ma L, Chang H, Chen L, Liu C, Xu J, Li J, Yan N (2012) Catal Sci Technol 2:915–917
27. Shu Y, Sun H, Quan X, Chen S (2012) J Phys Chem C 116:25319–25327
28. Chen L, Li J, Ge M, Ma L, Chang H (2011) Chin J Catal 32:836–841
29. Busca G, Larrubia MA, Arrighi L, Ramis G (2005) Catal Today 107–108:139–148
30. Zhang X, Shen Q, He C, Ma C, Cheng J, Li L, Hao Z (2012) ACS Catal 2:512–520